11-15-2021

# Lignin, sugar, and furan production of industrial hemp biomass via an integrated process

Jikai Zhao

Jason Griffin

Kraig Roozeboom

Juhee Lee

Donghai Wang

# Lignin, sugar, and furan production of industrial hemp biomass via an integrated process

Jikai Zhao[a], Jason Griffin[b], Kraig Roozeboom[c], Juhee Lee[d], Donghai Wang[a]*

[a]Carl and Melinda Helwig Department of Biological and Agricultural Engineering, Kansas State University, Manhattan, KS 66506, United States

[b]John C. Pair Horticultural Center, Department of Horticulture & Natural Resources, Kansas State University, Haysville, KS 67060, United States

[c]Department of Agronomy, Kansas State University, Manhattan, KS 66506, United States

[d]School of Public Policy, University of California, Riverside, CA 92521, United States

*Corresponding author: dwang@ksu.edu (Donghai Wang)

## Abstract

Traditional pretreatment of lignocellulosic biomass is often accompanied by washing and disposal of wastewater, which leads to overuse of water and loss of by-products. The objectives of this study were to validate the potential of an acid-base integrated process for simultaneous sugars, furans, and lignin production without washing and wastewater discarding. The difference in conversion performance among different biomass resources was also demonstrated. Parallel acetic acid (HOAc, pH=2.25) and sodium hydroxide (NaOH, pH=13.46) pretreatments followed by solid and liquid integration were applied to four genotypes of industrial hemp (*Cannabis sativa L.*) biomass that were harvested from two planting locations (Haysville and Manhattan, KS). Results showed that genotype, planting location, and their interaction had notable influences on biomass composition and its conversion to bioproducts but exhibited different trends. Glucan content of biomass from Haysville, ranging from 47.29-50.05%, were higher than those of 42.49-48.38% from Manhattan with the lowest being Vega (Manhattan) and the highest being Hlukouskii (Haysville). Xylan and lignin contents in all the hemp genotypes were 11.70-13.88% and 10.45-15.14%, respectively. The integration process effectively rendered the pH of the integrated filtrate and slurry to approximately 4.80. The highest lignin recovery of 73.13 g/kg biomass was achieved by Rigel from Manhattan. Fourier transform infrared spectroscopy (FTIR) characterization showed that only lignin derived from Vega (Haysville) and Anka (Manhattan) was comparable to the commercial alkali lignin. Retaining monosaccharides (2.24-3.81 g/L) enhanced sugar concentrations (glucose:

40.40-45.71 g/L; xylose: 7.09-8.88 g/L) and conversion efficiencies (glucose: 71.19-77.71%;

xylose: 45.42-52.03%). Besides, furans including 0.79-1.25 g/L of hydroxymethylfurfural

(HMF) and 0.99-1.59 g/L of furfural coupling with 1.96-2.95% and 10.00-14.65% conversion

efficiencies, respectively, were obtained in the final hydrolysate. Biomass from Haysville

produced relatively higher glucose concentrations than those from Manhattan. Based on mass

balance, the most productive genotype was Rigel. This study offers essential information to

reduce water and chemical overconsumption and to understand the effects of genotype and

planting location on biomass valorization.

## 1. Introduction

In past decades, the legislative limitation of industrial hemp (*Cannabis sativa L.*) cultivation and processing in Western Europe, the USA, and Canada, to inhibit its abuse and illegal utilization for drug production (Cherney and Small, 2016; Fike, 2016), remarkably weakened its economic importance. Therefore, industrial hemp is often recognized as an underdeveloped and underutilized crop. Currently, the USA federal restriction on industrial hemp cultivation is unlocked by the 2018 US farm bill that approved its cultivation with a delta-9 tetrahydrocannabinol content (THC) below 0.3% in 46 states (Adesso et al., 2019). Governing changes are leading to a resurgent commercial exploration of this crop. The chemical composition of hemp seed is of great interest, attributed to the potential for food and nutraceutical and pharmaceutical applications (Farinon et al., 2020; Wang and Xiong, 2019; Xu et al., 2021). Industrial hemp stover, either as a by-product of hemp grain production or as a primary product, could serve an important role as a biochemical and biofuel feedstock (Zhao et al., 2020a).

Compared to other lignocellulosic biomass such as wheat straw, corn stover, and sorghum biomass, industrial hemp biomass has been reported to contain higher cellulose content. Thus, it has the potential to be a competitive candidate for biomass-to-bioproducts production (Zhao et al., 2020a). To render industrial hemp biomass amenable to enzymatic hydrolysis, large numbers of pretreatment strategies such as acid, alkali, liquid hot water, steam, organosolv, and Microwave-assisted ionic liquids have been investigated by many research groups (de Vega and Ligero, 2017; George et al., 2015; Kamireddy et al., 2013; Kreuger et al., 2011; Kuglarz et al.,

65    2014; Väisänen et al., 2019; Viswanathan et al., 2020; Xie et al., 2017; Zhao et al., 2020a). In

66    this regard, excessive post-pretreatment washing was widely discerned to moderate the severity

67    of pH and inhibitory compounds in the pretreated biomass and filtrate (Das et al., 2020; Kreuger

68    et al., 2011; Kuglarz et al., 2014; Semhaoui et al., 2018). This process generates abundant

69    wastewater, which inevitably inhibits commercial exploration. Therefore, reducing water and

70    chemical consumption is highly needed for industrial hemp biomass valorization. To address this

71    issue, our previous study proved that integrating acid and alkali pretreated biomass and their

72    mixed filtrate for enzymatic hydrolysis was performed well without compromising sugar yield

73    (Zhao et al., 2021b). The neutralization of residual acid and alkali in the biomass and filtrate can

74    be achieved simultaneously during the integration process (Zhao et al., 2021b). Also, the

75    dissolved lignin in the alkaline filtrate can be recovered. The post-washing and chemical disposal

76    procedures can be avoided after pretreatment. Therefore, the major advantage of the acid-base

77    integration process is the feasibility to minimize water and chemical overconsumption. On the

78    other hand, Viswanathan, et al. (2021) investigated the economic perspectives of ethanol and

79    biodiesel coproduction from industrial hemp biomass (genotype of 19m96136) and found that

80    minimum selling prices of biodiesel ranged from $1.09 to $4.88/L when the ethanol selling price

81    was $0.62/L depending on the lipid content. Das et al. (2020) reported that dilute acid

82    pretreatment and enzymatic hydrolysis predicted practical ethanol yields of 264.98−344.47 L/dry

83    ton hemp stems with the highest ethanol yield of 344.85 L/dry ton hemp stems from the Futura

84    75 genotype. These studies indicate that industrial hemp biomass has the potential to be used for

85 biofuel production but the variation among genotypes and the effect of the growing environment

86 should be considered.

87     The effects of agronomical practices, genotypes, and cultivation sites on the nutritional,

88 phytochemical, and antioxidant properties of hempseed and pant growth performances and

89 biomass yields have been considerably explored (Ascrizzi et al., 2019; Campiglia et al., 2017;

90 Cappelletto et al., 2001; García-Tejero et al., 2019; Irakli et al., 2019; Pagnani et al., 2018;

91 Scheliga et al., 2018; Sraka et al., 2019; Struik et al., 2000). However, few studies have been

92 targeted at the impacts of genotype and environmental factors on the bioconversion of industrial

93 hemp biomass to lignin, sugar, and furan. In this respect, Das et al. (2020) compared the

94 potential of eleven industrial hemp biomass for biofuel and bioproducts production through

95 dilute sulfuric acid pretreatment coupled with theoretical simulation and found that

96 dual-purpose genotypes had advantages over fiber-only Genotypes in terms of potential per

97 hectare gross profit. Additionally, Zhao et al. (2020c) evaluated four varieties of industrial

98 hemp biomass to illuminate their variation for bioethanol production through liquid hot water,

99 sulfuric acid, and NaOH pretreatments. The two studies demonstrated the influence of

100 genotypes on biomass valorization, but environmental factors such as planting location remain

101 unanswered.

102     In this study, the integrated HOAc and NaOH pretreatments were applied to four

103 dual-purpose industrial hemp genotypes grown at two planting locations. The objective of this

104 research was to demonstrate the effects of genotype and planting location on industrial hemp

105  biomass valorization using an integrated biomass pretreatment method. Thus, effects of

106  genotype, planting location, and their interaction on the chemical composition of biomass and

107  filtrate as well as chemical (glucose, xylose, HMF, furfural, and lignin) conversion

108  performances were elucidated. The recovered lignin was also compared with commercial alkali

109  lignin. Additionally, relationships between biomass composition and its conversion

110  performances to bioproducts were demonstrated. This study offers essential information to

111  understand the effects of genotype and planting location on biomass-to-chemicals production

112  and promote industrial exploration with limited water and chemical consumption.

113

## 2. Materials and Methods

### 2.1 Industrial hemp cultivation and materials

116  Stover remaining after threshing to remove grain from whole-plant samples of four

117  dual-purpose genotypes of industrial hemp (Anka, Rigel, Vega, and Hlukouskii 51) that were

118  harvested from two planting locations (Haysville and Manhattan, KS) were used for this study.

119  Field management details can be found in Griffin et al. (2020). The detailed weather data in

120  Haysville and Manhattan for May-September of 2020 are shown in Fig. 1. Growing conditions

121  were generally favorable for hemp growth at both locations, but the Haysville location had a

122  shallower, more coarse soil [Canadian-Waldeck fine sandy loam (coarse-loamy, mixed,

123  superactive, thermic Udic-Fluvaquentic Haplustoll)], compared to the Manhattan location

124  [Wymore silty clay loam (fine, smectitic, mesic Aquertic Argiudoll)]. Overall, from May to

125 September, the average relative humidity was 70.44% for Manhattan and 72.36% for Haysville,

126 the total precipitation was 498.58 mm for Manhattan and 410.19 mm for Haysville, and the

127 average of solar radiation was 20.80 MJ/m$^2$ for Manhattan and 20.57 MJ/m$^2$ for Haysville.

128 Supplemental irrigation was applied during a dry period in June, soon after planting at Haysville

129 to facilitate stand establishment and early growth. Substantial rainfall events in the first half of

130 August likely minimized the negative impacts of a dry period in the second half of the month at

131 both locations. Vegetative growth was essentially complete at that point, so the dry period likely

132 had a minimal impact on biomass accumulation and composition but may have affected seed fill

133 and composition at both locations.

134 The small branches and leaves of received hemp biomass were removed from the stems, and

135 only the stems were used for analysis. Stems were sequentially ground by SM 2000 cutting mill

136 (Restsch Inc. Newton, PA) and kitchen mill (Blendtec Residential, Orem, UT) for size reduction

137 (< 2 mm). After grinding, the samples were stored in Ziploc bags at room temperature before

138 further use. Alkali lignin (370959-100G) was purchased from Sigma-Aldrich chemicals

139 company (St. Louis, MO). Cellic® CTec3 (cellulase, 516 mg/mL) and NS22244 (hemicellulase,

140 266 mg/mL) were obtained from Novozymes (Franklinton, NC).

141

142 **2.2 Biomass pretreatment and integration process**

143 Biomass pretreatment was carried out in a sandbath (Techne Inc., Princeton, NJ) with

144 continuous air blast. Four-gram biomass was loaded into the 75 mL stainless steel reactors

145 (Swagelok, Kansas City Valve & Fitting Co., KS), followed by adding 40 mL HOAc (pH=2.25)

or NaOH (pH=13.46) reagents. The selected pHs of these reagents were based on the results of the pre-experiment. After manual mingling, these reactors were instantly submerged into the sandbath at 190 °C. When pretreatment time reached 40 min, these reactors were quenched by cold tap water to avoid the further reaction. The pretreated slurry was separated into solid and filtrate by vacuum filtration coupled with Whatman filter paper. The pH values were measured in situ by an Orion Star™ A211 Benchtop pH Meter (Thermo Fisher Scientific Inc., Waltham, MA). It must be mentioned that HOAc and NaOH pretreated biomass were not subjected to post-washing.

**2.3 Enzymatic hydrolysis**

After pretreatment, HOAc and NaOH pretreated filtrates were mixed with slow shaking to precipitate the lignin and then subjected to vacuum filtration. Whereas HOAc pretreated biomass was directly mixed with NaOH pretreated biomass in the 250 mL Erlenmeyer flasks and then added the above-integrated filtrate. To verify the neutralization of residual HOAc and NaOH in solid residues, the pH of the integrated slurry was examined. Enzymatic hydrolysis was initiated by pipetting 100 µL cellulase/g biomass and 50 µL hemicellulase/g biomass (Zhao et al., 2021a). These flasks were transferred into an orbital shaker (I2400 Incubator Shaker, New Brunswick, USA) at 49 °C with 160 rpm for 72 h. Herein, no pH adjusting for the integrated slurry was carried out.

## 2.4 Analytical methods

The chemical composition of raw industrial hemp biomass was measured according to the National Renewable Energy Laboratory (NREL) (Sluiter et al., 2008ab). The extracted biomass (~ 0.3000 g) was mixed with 3 mL of 72% sulfuric acid and stirred in a 30 °C water bath for 60 min. After that, 84 mL of deionized water was added to reduce the sulfuric acid concentration to 4%, and the sealed flask was then autoclaved at 121 °C for 60 min. The flask was cooled down at room temperature and filtered by a pre-weighed filter crucible. The 1.5 mL filtrate was pipetted for acid-soluble lignin (ASL) test, and 10 mL filtrate was first neutralized with 0.40 g calcium carbonate for 40 min and filtered for glucose and xylose determination. Finally, solid residue in the crucible was washed with at least 50 mL distilled water and dried overnight at 105 °C for acid-insoluble lignin (AIL) test. After that, the crucible was shifted into the Muffle furnace at 575 °C for the ash test. Monosaccharides (glucose and xylose), furfural, and HMF in the filtrate were determined by a 1260 high-performance liquid chromatography (HPLC) system (Agilent, Santa Clara, CA). The measurement parameters were: an HPX-87H organic acid column (7.8×300 mm) was a separation column and set at 60 °C; 0.005 M sulfuric acid was mobile phase buffer with a flow rate of 0.6 mL/min; the refractive index detector temperature was set at 45 °C (Zhao et al., 2021a). Chemical bonds of raw hemp biomass were identified by a 400 FTIR spectrophotometer (PerkinElmer Corp., Shelton, CT) equipped with a room temperature deuterated lanthanum α alanine doped triGlycine sulphate (RT-DLαTGS) detector. Background scanning was carried out for calibration before determination. The parameters such as 4000-400 cm$^{-1}$ wavenumber range, 4 cm$^{-1}$ resolution, 68-71 pressure intensity, and 32 scans per sample

187 were applied (Zhao et al., 2020c). Besides, glucose, xylose, HMF, and furfural conversion

188 efficiencies were calculated as shown in Eqs (1) to (4), while glucose, xylose, HMF, and furfural

189 yields based on the initial raw biomass weight were calculated as shown in Eqs (5) to (8). These

190 equations were referred to our previous studies (Zhao et al., 2021a, 2020b).

191
$$E_{(g)} = \frac{C_{(glucose)} \times V_{(mL)} \div 1000}{M_{(b)} \times C_{(glucan)} \div 0.9} \times 100\% \quad (1)$$

192
$$E_{(x)} = \frac{C_{(xylose)} \times V_{(mL)} \div 1000}{M_{(b)} \times C_{(xylan)} \div 0.88} \times 100\% \quad (2)$$

193
$$E_{(HMF)} = \frac{C_{(HMF)} \times V_{(mL)} \div 1000 \div MM_{(HMF)} \times MM_{(glucose)}}{M_{(b)} \times C_{(glucan)} \div 0.9} \times 100\% \quad (3)$$

194
$$E_{(furfural)} = \frac{C_{(furfural)} \times V_{(mL)} \div 1000 \div MM_{(furfural)} \times MM_{(xylose)}}{M_{(b)} \times C_{(xylan)} \div 0.88} \times 100\% \quad (4)$$

195
$$Y_{(g)} = \frac{C_{(glucose)} \times V_{(mL)} \div 1000}{M_{(b)}} \quad (5)$$

196
$$Y_{(x)} = \frac{C_{(xylose)} \times V_{(mL)} \div 1000}{M_{(b)}} \quad (6)$$

197
$$Y_{(HMF)} = \frac{C_{(HMF)} \times V_{(mL)} \div 1000}{M_{(b)}} \quad (7)$$

198
$$Y_{(furfural)} = \frac{C_{(furfural)} \times V_{(mL)} \div 1000}{M_{(b)}} \quad (8)$$

199 $E_{(g)}$, $E_{(x)}$, $E_{(HMF)}$, and $E_{(furfural)}$ are glucan-to-glucose, xylan-to-xylose, glucose-to-HMF, and

200 xylose-to-furfural conversion efficiencies, respectively. $Y_{(g)}$, $Y_{(x)}$, $Y_{(HMF)}$, and $Y_{(furfural)}$ are

201  glucose, xylose, HMF, and furfural yields, respectively. $C_{(glucose)}$, $C_{(xylose)}$, $C_{(HMF)}$, and $C_{(furfural)}$ are

202  glucose, xylose, HMF, and furfural concentrations (g/L) in the slurry, respectively. $M_{(b)}$ and

203  $V_{(mL)}$ are dry-basis solid weight and slurry volume, respectively. $C_{(glucan)}$ and $C_{(xylan)}$ are glucan

204  and xylan contents in raw hemp biomass before pretreatment, respectively. $MM_{(HMF)}$, $MM_{(glucose)}$,

205  $MM_{(furfural)}$, and $MM_{(xylose)}$ are the molar mass of HMF, glucose, furfural, and xylose, respectively.

206  0.9 and 0.88 are the transformation factor of glucan-to-glucose and xylan-to-xylose, respectively.

207

208  **2.5. Statistical analysis**

209      In order to elucidate the effects of genotype, planting location, and their interaction on the

210  chemical composition of biomass and filtrate as well as chemical conversion performances,

211  multivariate analysis of variance (ANOVA) was performed using IBM SPSS Statistics Version

212  27.0 (Armonk, NY, IBM Corp). In this regard, the genotype and planting location were treated

213  as fixed factors, other variables such as glucose concentration and conversion efficiency were

214  recognized as dependent variables. Means for significant difference were identified using the

215  least significant difference method.

216

217  **3. Results and discussion**

218  **3.1 Chemical composition of industrial hemp biomass**

219      Effects of genotype, planting location, and their interaction on the chemical composition of

220  industrial hemp biomass are summarized in Table 1. It is clear that genotype played a significant

221   role in determining glucan, xylan, ASL, and extractives, whereas planting location had

222   significant effects on glucan and lignin components. This is comparable with the finding that

223   planting location had significant effects on the chemical compositions of big bluestem (Zhang et

224   al., 2012). However, it is unexpected that the interaction between genotype and planting location

225   had a significant influence only on extractives (Table 1). Glucan content of biomass from

226   Haysville ranged from 47.29-50.05%, which were relatively higher than those (42.49-48.38%)

227   from Manhattan (Fig. 2A). Vega from Manhattan exhibited the lowest glucan content of 42.49%,

228   while Hlukouskii from Haysville showed the highest glucan content of 50.05% (Fig. 2A). It can

229   be recognized that roughly compared to grain straws (31-39%) (Tian et al., 2018) and corn stover

230   (31.0-41.2%) (Zhao et al., 2020a), industrial hemp biomass obtained from this work was

231   composed of higher glucan content. Xylan content for all the genotypes fell in the range of

232   11.70-13.88% with the lowest xylan content being Hlukouskii from Haysville and the highest

233   xylan content being Rigel from Manhattan (Fig. 2A). Total carbohydrates (glucan and xylan)

234   accounted for 56-63%. These results are comparable to the previous studies, where different

235   genotypes of industrial hemp biomass were investigated (Xu et al., 2016; Zhao et al., 2020a).

236   The lignin content of industrial hemp biomass has been reported to differ dramatically from 15 to

237   30%, depending on the genotypes (Xu et al., 2016). In this work, it was noticed that there was a

238   slight variation in ASL (0.47-0.50%) and AIL (9.96-14.67%) lignin content among the biomass

239   samples, with the total lignin content ranging from 10.45 to 15.14%. Extractives of four

240   industrial hemp biomass ranged from 11.63 to 18.36% (Fig. 2A). In contrast, Das et al. (2020)

241   reported that eleven industrial hemp biomass genotypes contained 43.8-50.1% of glucan,

242  11.6-14.2% of xylan, 15.4-29.4% of lignin, and 5.5-11.9% of extractives. Additionally, the

243  differences in chemical bonds among the four industrial hemp biomass harvested at Haysville

244  and Manhattan were characterized by FTIR spectrum (Fig. 2B). It was found that peaks at 1590

245  $cm^{-1}$ (C=C stretching from aromatic skeletal vibration) and 1514 $cm^{-1}$ (aromatic skeleton of

246  lignin) in Rigel from Manhattan were slightly more intense than biomass from other genotypes

247  and locations (Fig. 2B). It is consistent with the relatively higher lignin content (Fig 2A). It was

248  also noticed that other peaks showed no visible variations among the biomass samples (Fig. 2B).

249

250  **3.2 pH and chemical composition of filtrate**

251  Due to the severer pH of acid and alkali pretreated filtrate comparing to buffer, adequate

252  water washing followed by direct wastewater discarding was generally observed (de Vega and

253  Ligero, 2017; Pagnani et al., 2018; Xie et al., 2017). For example, a previous study reported that

254  160 mL water/g raw biomass was required to clarify the waste liquor from NaOH and

255  hydrothermal pretreatment of coconut fiber and reduce their pH to neutral (da Costa Nogueira et

256  al., 2018). Herein, mixing the HOAc and NaOH pretreated filtrate was performed to utilize it as a

257  buffer.

258  It was found that genotype, planting location, and interaction between genotype and

259  planting location had significant effects on the pH of filtrate (Table 1). The initial pHs for HOAc

260  and NaOH reagents used for biomass pretreatment were 2.25 and 13.46, respectively. After

261  pretreatment, the pretreated filtrate showed slight variations in terms of pH, ranging from 2.91 to

262  2.99 (HOAc) and 12.96 to 13.15 (NaOH) for biomass from Haysville and from 3.03 to 3.08

263  (HOAc) and 13.05 to 13.20 (NaOH) for biomass from Manhattan (Fig. 3). The slight variation in

264  pH is attributed to the heterogeneous distribution of hemicellulose among different biomass

265  samples (Zhao et al., 2020b). Compared to the starting pH of reagents, the mitigation of pH in

266  the filtrate is also attributed to the dilution caused by adding biomass. As mentioned above, the

267  resultant filtrate with the extreme pH is unable to be utilized for efficient enzymatic hydrolysis.

268  However, the pH severity was attenuated through the integration of HOAc and NaOH pretreated

269  filtrate (Fig. 3), as the pHs of the integrated filtrate were 4.78-4.82 for biomass from Haysville

270  and 4.79-4.92 for biomass from Manhattan (Fig. 3), indicating that a neutralization reaction was

271  performed between acids and NaOH in the filtrate. Furthermore, the black liquor obtained from

272  NaOH pretreatment turned into a brown color, when it was mixed with HOAc pretreated filtrate

273  with the precipitation of lignin. In comparison to the complicated and high-cost

274  poly(ether)sulfone-based ultrafiltration membrane filter (Kim et al., 2020), this simple

275  integration process might be more feasible to alleviate the pH of filtrate and utilize the residual

276  chemicals.

277      The monosaccharides derived from HOAc and NaOH pretreatments of four genotypes of

278  hemp biomass in the filtrate were tracked by HPLC (Fig. 4). A comparison of sugar

279  concentrations in the pretreated filtrate often discloses the variances in the biomass recalcitrance

280  (Zhao et al., 2021a). For HOAc pretreatment, the highest and lowest glucose concentration of

281  1.77 g/L and 0.77 g/L was generated by Rigel from Haysville and Vega from Manhattan,

282  respectively (Fig. 4 A and B), and the highest and lowest xylose concentration of 4.82 g/L and

283     2.16 g/L was obtained by Hlukouskii and Rigel from Manhattan, respectively (Fig. 4B). In the

284     case of NaOH pretreatment, no glucose was found in the filtrate for Anka from Haysville or

285     Anka and Vega from Manhattan (Fig. 4A and B). Carbohydrates of biomass are more susceptible

286     to confront the pretreatment with acid rather than NaOH reagent (Zhao et al., 2020b), which is in

287     agreement with the finding that HOAc pretreatment showed 0.16-1.12 g/L of glucose and

288     1.43-4.41 g/L of xylose higher than NaOH pretreatment (Fig. 4A and B). Based on the high

289     sugar concentrations in the filtrate, direct disposal can certainly cause sugar loss. The final

290     glucose and xylose concentrations in the integrated filtrate ranged from 0.84 to 1.64 g/L and 1.31

291     to 2.55 g/L, respectively, depending on the genotype and planting location of industrial hemp

292     biomass (Fig. 4A and B).

293     Due to the inhibitory compounds, physical, chemical, and biological technologies

294     including membrane filtration, neutralization reaction, and activated charcoal adsorption have

295     been promoted to render biomass filtrate amenable to enzymes and microbes (Kumar et al.,

296     2020). Furfural and HMF, decomposed from hemicellulose and cellulose, respectively, are

297     mainly recognized to inhibit microbial growth. Unlocked lignin units were informed to absorb

298     on the surfaces of cellulose and hemicellulose tightly to circumvent enzymatic accessibility (Li

299     et al., 2018). Also, lignin-derived phenolic compounds can bring a severe inhibitory effect on

300     enzymatic hydrolysis (Chen et al., 2020) and lead to incompatibility of biological membranes

301     (Jung and Kim, 2017). It was discerned that HMF and furfural in HOAc pretreated filtrate

302     ranged from 1.69 to 2.41 g/L and from 2.51 to 3.68 g/L, respectively (Fig. 4). The highest HMF

303 and furfural concentration was acquired by Hlukouskii and Rigel from Haysville (Fig. 4A), and

304 the lowest HMF and furfural concentration was obtained by Anka and Hlukouskii from

305 Manhattan (Fig. 4B). However, NaOH pretreatment prompted no HMF and furfural formation

306 in the filtrate (Fig. 4A and B). After integration, the concentrations of sugar-derived inhibitors

307 that originated from the HOAc pretreated filtrate were relieved: HMF and furfural were in the

308 range of 0.71-0.95 g/L and 0.64-1.25 g/L, respectively (Fig. 4A and B). These results indicate

309 that this simple integration approach is multipurpose to associate the strengths of acid-base

310 pretreatments and to solve the bottleneck of inhibitors in a practical path.

311

312 **3.3 Lignin recovery and FTIR characteristic**

313      Tremendous attention has been attracted to reduce the resistance of biomass and enhancing

314 its accessibility to enzymes and microorganisms, while additional byproducts, especially lignin,

315 have rarely been recovered qualitatively (Huang et al., 2020). However, the conversion of

316 biomass-based lignin to polymeric materials might offer potential values for biomass upgrades

317 (Upton and Kasko, 2016). In this work, the lignin was precipitated after integrating HOAc and

318 NaOH pretreated filtrate and then subjected to vacuum filtration and oven drying. Lignin

319 recoveries based on raw biomass and its FTIR characteristics are compared with commercial

320 alkali lignin as a control (Fig. 5). It was found that planting location and interaction between

321 genotype and planting location showed significant effects on lignin recovery (Table 2). Industrial

322 hemp biomass could be differentiated in terms of its lignin recovery: 50.63-57.50 g lignin per kg

323     biomass from Haysville, 56.88-73.13 g lignin per kg biomass from Manhattan, and Rigel being

324     the highest from Manhattan (Fig. 5A).

325      The FTIR spectrum of the isolated lignin fraction was compared with commercial alkali

326     lignin. For biomass from Haysville, only Vega showed similar intensities of peaks at 1592 and

327     1506 cm$^{-1}$ (assigned to the vibration of aromatic rings), 1461 cm$^{-1}$ (assigned to the methoxyl C-H

328     bending and C-C stretching in the aromatic skeleton), 1265 cm$^{-1}$ (assigned to the aromatic C-O

329     stretching of syringyl units and/or condensed guaiacyl units), 1120 cm$^{-1}$ (assigned to the syringyl

330     units), 1030 cm$^{-1}$ (assigned to C-OH and C-O-C stretching of the side groups and glycosidic

331     bonds), and 830 cm$^{-1}$ (assigned to the guaiacyl units) with the commercial alkali lignin (Fig. 5A).

332     For biomass from Manhattan, only Anka exhibited analogous intensities of peaks at 1592, 1506,

333     1120, 1030, and 830 cm$^{-1}$ compared to the commercial alkali lignin (Fig. 5A). These results

334     indicate that lignin derived from Vega (Haysville) and Anka (Manhattan) might have comparable

335     chemical structures with the commercial alkali lignin.

336

337     **3.4 Enzymatic hydrolysis of integrated biomass and filtrate**

338      Rinsing pretreated biomass with adequate water, followed by adding a fresh buffer solution

339     (sodium acetate, citrate, and phosphate), has been typically applied for enzymatic hydrolysis.

340     This conventional process inevitably causes solid-liquid imbalance, especially resulting in the

341     accumulation of wastewater. Herein, we emphasize that HOAc and NaOH pretreated solid

342     biomass were first mixed without post-washing, and the integrated filtrate was loaded and

343     homogeneously stirred without pH adjusting. As expected, the neutralization reaction also

344 happened between the HOAc and NaOH pretreated biomass, evidenced by the final slurry pHs

345 ranging from 4.60 to 4.65 for biomass from Haysville and from 4.65 to 4.70 for biomass from

346 Manhattan (Fig. 6A). Thus, the resulting pH is suitable for enzymatic hydrolysis without pH

347 adjusting and new buffer solution addition, avoiding wastewater discarding and extra chemical

348 consumption. Besides, planting location and interaction between genotype and planting location

349 had significant influences on the pH of the integrated slurry (Table 1).

350      After enzymatic hydrolysis, the slurry was subjected to centrifugal separation to segregate

351 solid from hydrolysates. The chemical concentrations were quantitatively determined by HPLC

352 (Fig. 6B), and their conversion efficiencies and yields were calculated as shown in Table 3. It

353 was observed that genotype, planting location and their interaction exhibited significant impacts

354 on chemical conversion performances (Table 2). Industrial hemp biomass from Haysville

355 reached glucose concentrations of 41.97-45.71 g/L, which were slightly higher than those from

356 Manhattan (40.40-44.38 g/L) (Fig. 4B), but there was no similar trend found for

357 glucan-to-glucose conversion efficiencies: 72.97-75.33% and 71.19-77.71% for industrial hemp

358 biomass from Haysville and Manhattan, respectively (Table 3). The highest glucose

359 concentration and conversion efficiency were achieved by Hlukouskii (45.71 g/L) from

360 Haysville and Vega (77.71%) from Manhattan, respectively. In terms of xylose, the integration

361 process attained xylose concentrations of 7.09-8.88 g/L (Fig. 6B), with their conversion

362 efficiencies of 45.42-52.03% (Table 3). The highest xylose concentration and conversion

363 efficiency were achieved by Rigel (8.88 g/L) from Manhattan and Hlukouskii (52.03%) from

364 Haysville, respectively. In contrast, Das et al. (2020) reported that dilute sulfuric acid

365 pretreatment of eleven industrial hemp biomass only reached 30% of xylose conversion

366 efficiencies (maximum potential based on raw biomass). On the other hand, HMF (0.79-1.25 g/L)

367 and furfural (0.99-1.59 g/L) were remained in the final hydrolysates (Fig. 4B), corresponding

368 with 1.96-2.95% (maximum potential based on glucose-to-HMF) and 10.00-14.65% (maximum

369 potential based on xylose-to-furfural) conversion efficiencies, respectively (Table 3). Regarding

370 the conversion performance based on raw biomass, sugar concentration and conversion

371 efficiencies obtained in the present work were superior to those in the previous report (Zhao et

372 al., 2020a), where industrial hemp biomass pretreated by steam, sulfuric acid, or NaOH was

373 subjected to remarkable water washing and drying, followed by enzymatic hydrolysis with new

374 buffer solution under low (7.5% <) solid loading. The chemical yields (g/kg biomass) based on

375 the raw biomass were also summarized in Table 3. Given 1.0 kg of raw dried biomass used for

376 HOAc (500 g) and NaOH (500 g) pretreatments, 366.85-418.89 g of glucose, 64.04-80.84 g of

377 xylose, 7.14-11.46 g of HMF, and 8.94-14.53 g of furfural could be obtained, in addition to

378 50.63-73.13 g of lignin. Among the four genotypes harvested from Haysville and Manhattan, the

379 most and least productive genotype is Rigel and Vega, respectively (Table 3).

380

381 **3.5 Relationship between biomass composition and chemical conversion performance**

382     To our knowledge, this is the first report on studying the relationship between chemical

383 composition (glucan, xylan, and lignin) of raw biomass and the concentration and conversion

384 efficiency of hydrolysates (glucose, xylose, HMF, and furfural), although a previous study by Xu

385 et al. (2016) reported that glucan and lignin contents in the ionic liquid pretreated rice straw had

a positive linear correlation and negative linear correlation with sugar digestibility. Herein, it was observed that glucan content showed a positive linear correlation ($r = 0.81$) with glucose concentration (Fig. 7A), xylan content showed a positive linear correlation ($r = 0.72$) with furfural concentration (Fig. 7B), and lignin content showed a negative linear correlation ($r = -0.73$) with HMF concentration (Fig. 7C). Das et al. (2020) found no obvious correlation between lignin content and sugar conversion efficiencies among the eleven hemp biomass that had notable variation in lignin contents. Besides, glucan content had a moderate correlation ($r = 0.65$) with HMF concentration; lignin content had a moderate correlation ($r = 0.67$) with HMF conversion efficiency; glucose conversion efficiency had a moderate correlation ($r = -0.58$) with furfural concentration and conversion efficiency; xylose conversion efficiency had moderate correlation with glucose concentration ($r = 0.60$), xylose concentration ($r = 0.53$), and HMF concentration ($r = 0.54$); and glucose concentration had a moderate correlation ($r = 0.61$) with HMF concentration (Fig. 7D). This relatively weak correlation between the composition of raw industrial hemp biomass and chemical conversion parameters indicates that non-quantitative factors are playing a role in the biomass-to-chemicals conversion interdependently.

## 4. Conclusion

Parallel HOAc and NaOH pretreatments with solid and liquid integration were demonstrated to produce glucose, xylose, HMF, furfural, and lignin without washing and wastewater discarding. Genotypes and planting locations had significant effects on bioproduct conversion performances. Industrial hemp biomass harvested from Haysville had relatively higher glucan

contents (47.29-50.05%) than those (42.49-48.38%) from Manhattan. Integrating HOAc and NaOH integrated filtrate reached the pH of 4.78-4.92, precipitating the soluble lignin (50.63-73.13 g/kg biomass). The recovered lignin from Vega (Haysville) and Anka (Manhattan) showed almost comparable FTIR characteristics with the commercial alkali lignin. Combining HOAc and NaOH pretreated biomass and their mixed filtrate for enzymatic hydrolysis achieved 40.40-45.71 g/L of glucose and 7.09-8.88 g/L of xylose. Besides, high-value HMF (0.79-1.25 g/L) and furfural (0.99-1.59 g/L) remained in the final hydrolysate. The higher glucose (71.19-77.71%) and xylose (45.42-52.03%) conversion efficiencies validate the potential of this integrated process to reduce water and chemical consumption. Based on mass balance, the most and least productive genotypes were Rigel and Vega, respectively. Glucan and xylan contents in the biomass showed a positive linear correlation with glucose and furfural concentration, respectively; whereas lignin content showed a negative linear correlation with HMF concentration. Additionally, increasing the solid loading of biomass and screening of low-cost acidic catalysts for pretreatment could be new perspectives for further explorations.

**CRediT authorship contribution statement**

Jikai Zhao: experimental implementation, data interpretation, and manuscript writing; Jason Griffin: industrial hemp biomass providing and manuscript revision; Kraig Roozeboom: industrial hemp biomass providing and manuscript revision; Juhee Lee: statistical analysis and manuscript revision; Donghai Wang: supervision and manuscript revision.

**Declaration of Competing Interest**

The authors declare that they have no known competing financial interests or personal relationships that could have appeared to influence the work reported in this paper.

437    **References:**

438    Adesso, M., Laser, P., Mills, A., 2019. An Overview of Industrial Hemp Law in the United States.

439        Univ. Dist. Columbia Law Rev. 22.

440    Ascrizzi, R., Ceccarini, L., Tavarini, S., Flamini, G., Angelini, L.G., 2019. Valorisation of hemp

441        inflorescence after seed harvest: Cultivation site and harvest time influence agronomic

442        characteristics and essential oil yield and composition. Ind. Crops Prod. 139, 111541.

443        https://doi.org/10.1016/j.indcrop.2019.111541

444    Campiglia, E., Radicetti, E., Mancinelli, R., 2017. Plant density and nitrogen fertilization affect

445        agronomic performance of industrial hemp (Cannabis sativa L.) in Mediterranean

446        environment. Ind. Crops Prod. 100, 246–254. https://doi.org/10.1016/j.indcrop.2017.02.022

447    Cappelletto, P., Brizzi, M., Mongardini, F., Barberi, B., Sannibale, M., Nenci, G., Poli, M., Corsi,

448        G., Grassi, G., Pasini, P., 2001. Italy-grown hemp: Yield, composition and cannabinoid

449        content. Ind. Crops Prod. 13, 101–113. https://doi.org/10.1016/S0926-6690(00)00057-1

450    Chen, X., Zhai, R., Li, Y., Yuan, X., Liu, Z.H., Jin, M., 2020. Understanding the structural

451        characteristics of water-soluble phenolic compounds from four pretreatments of corn stover

452        and their inhibitory effects on enzymatic hydrolysis and fermentation. Biotechnol. Biofuels

453        13, 1–13. https://doi.org/10.1186/s13068-020-01686-z

454    Cherney, J.H., Small, E., 2016. Industrial hemp in North America: Production, politics and

455        potential. Agronomy 6. https://doi.org/10.3390/agronomy6040058

456     da Costa Nogueira, C., de Araújo Padilha, C.E., de Sá Leitão, A.L., Rocha, P.M., de Macedo,

457         G.R., dos Santos, E.S., 2018. Enhancing enzymatic hydrolysis of green coconut

458         fiber—Pretreatment assisted by tween 80 and water effect on the post-washing. Ind. Crops

459         Prod. 112, 734–740. https://doi.org/10.1016/j.indcrop.2017.12.047

460     Das, L., Li, W., Dodge, L.A., Stevens, J.C., Williams, D.W., Hu, H., Li, C., Ray, A.E., Shi, J.,

461         2020. Comparative Evaluation of Industrial Hemp Cultivars: Agronomical Practices,

462         Feedstock Characterization, and Potential for Biofuels and Bioproducts. ACS Sustain. Chem.

463         Eng. 8, 6200–6210. https://doi.org/10.1021/acssuschemeng.9b06145

464     de Vega, A., Ligero, P., 2017. Formosolv fractionation of hemp hurds. Ind. Crops Prod. 97, 252–

465         259. https://doi.org/10.1016/j.indcrop.2016.12.021

466     Farinon, B., Molinari, R., Costantini, L., Merendino, N., 2020. The seed of industrial hemp

467         (*Cannabis sativa L.*): Nutritional quality and potential functionality for human health and

468         nutrition. Nutrients 12, 1–60. https://doi.org/10.3390/nu12071935

469     Fike, J., 2016. Industrial Hemp: Renewed Opportunities for an Ancient Crop. CRC. Crit. Rev.

470         Plant Sci. 35, 406–424. https://doi.org/10.1080/07352689.2016.1257842

471     García-Tejero, I.F., Durán Zuazo, V.H., Sánchez-Carnenero, C., Hernández, A., Ferreiro-Vera, C.,

472         Casano, S., 2019. Seeking suitable agronomical practices for industrial hemp (*Cannabis*

473         *sativa L.*) cultivation for biomedical applications. Ind. Crops Prod. 139, 111524.

474         https://doi.org/10.1016/j.indcrop.2019.111524

475    George, M., Mussone, P.G., Bressler, D.C., 2015. Improving the accessibility of hemp fibres

476        using caustic to swell the macrostructure for enzymatic enhancement. Ind. Crops Prod. 67,

477        74–80. https://doi.org/10.1016/j.indcrop.2014.10.043

478    Griffin, J., Roozeboom, K., Haag, L., Shelton, M., Wilson, C., Myers, T., 2020. 2019 Kansas

479        State University Industrial Hemp Dual-Purpose and Fiber Trial. Kansas Agric. Exp. Stn. Res.

480        Reports 6. https://doi.org/10.4148/2378-5977.7882

481    Huang, D., Li, R., Xu, P., Li, T., Deng, R., Chen, S., Zhang, Q., 2020. The cornerstone of

482        realizing lignin value-addition: Exploiting the native structure and properties of lignin by

483        extraction methods. Chem. Eng. J. 402, 126237. https://doi.org/10.1016/j.cej.2020.126237

484    Irakli, M., Tsaliki, E., Kalivas, A., Kleisiaris, F., Sarrou, E., Cook, C.M., 2019. Effect of genotype

485        and growing year on the nutritional, phytochemical, and antioxidant properties of industrial

486        hemp      (*Cannabis sativa L.*)     seeds.     Antioxidants    8,    20–25.

487        https://doi.org/10.3390/antiox8100491

488    Jung, Y.H., Kim, K.H., 2017. Evaluation of the main inhibitors from lignocellulose pretreatment

489        for enzymatic hydrolysis and yeast fermentation. BioResources 12, 9348–9356.

490        https://doi.org/10.15376/biores.12.4.9348-9356

491    Kamireddy, S.R., Li, J., Abbina, S., Berti, M., Tucker, M., Ji, Y., 2013. Converting forage

492        sorghum and sunn hemp into biofuels through dilute acid pretreatment. Ind. Crops Prod. 49,

493        598–609. https://doi.org/10.1016/j.indcrop.2013.06.018

494     Kim, S., Kim, S.D., Sohn, S.Y., 2020. Evaluation of the wastewater generated during alkaline

495     pretreatment of biomass for feasibility of recycling and reusing. Renew. Energy 155, 1156–

496     1164. https://doi.org/10.1016/j.renene.2020.04.018

497     Kreuger, E., Sipos, B., Zacchi, G., Svensson, S.E., Björnsson, L., 2011. Bioconversion of

498     industrial hemp to ethanol and methane: The benefits of steam pretreatment and

499     co-production.          Bioresour.          Technol.          102,          3457–3465.

500     https://doi.org/10.1016/j.biortech.2010.10.126

501     Kuglarz, M., Gunnarsson, I.B., Svensson, S.E., Prade, T., Johansson, E., Angelidaki, I., 2014.

502     Ethanol production from industrial hemp: Effect of combined dilute acid/steam pretreatment

503     and        economic        aspects.        Bioresour.        Technol.        163,        236–243.

504     https://doi.org/10.1016/j.biortech.2014.04.049

505     Kumar, V., Yadav, S.K., Kumar, J., Ahluwalia, V., 2020. A critical review on current strategies

506     and trends employed for removal of inhibitors and toxic materials generated during biomass

507     pretreatment.          Bioresour.          Technol.          299,          122633.

508     https://doi.org/10.1016/j.biortech.2019.122633

509     Li, X., Li, M., Pu, Y., Ragauskas, A.J., Klett, A.S., Thies, M., Zheng, Y., 2018. Inhibitory effects

510     of lignin on enzymatic hydrolysis: The role of lignin chemistry and molecular weight.

511     Renew. Energy 123, 664–674. https://doi.org/10.1016/j.renene.2018.02.079

512     Pagnani, G., Pellegrini, M., Galieni, A., D'Egidio, S., Matteucci, F., Ricci, A., Stagnari, F., Sergi,

513     M., Lo Sterzo, C., Pisante, M., Del Gallo, M., 2018. Plant growth-promoting rhizobacteria

514     (PGPR) in Cannabis sativa 'Finola' cultivation: An alternative fertilization strategy to

515     improve plant growth and quality characteristics. Ind. Crops Prod. 123, 75–83.

516     https://doi.org/10.1016/j.indcrop.2018.06.033

517 Scheliga, M., Brand, U., Türk, O., Gruber, S., Medina, L., Petersen, J., 2018. Yield and quality of

518     bast fibre from *Abutilon theophrasti* (Medic.) in southwest Germany depending on the site

519     and fibre extraction method. Ind. Crops Prod. 121, 320–327.

520     https://doi.org/10.1016/j.indcrop.2018.05.014

521 Semhaoui, I., Maugard, T., Zarguili, I., Rezzoug, S.A., Zhao, J.M.Q., Toyir, J., Nawdali, M.,

522     Maache-Rezzoug, Z., 2018. Eco-friendly process combining acid-catalyst and

523     thermomechanical pretreatment for improving enzymatic hydrolysis of hemp hurds.

524     Bioresour. Technol. 257, 192–200. https://doi.org/10.1016/j.biortech.2018.02.107

525 Sluiter, A., Hames, B., Ruiz, R., Scarlata, C., Sluiter, J., Templeton, D., and C., D., 2008.

526     Determination of Structural Carbohydrates and Lignin in Biomass: Laboratory Analytical

527     Procedure (LAP); Issue Date: April 2008; Revision Date: July 2011 (Version 07-08-2011) -

528     42618.pdf. Tech. Rep. NREL/ TP -510 -42618 1–15.

529 Sluiter, A., Ruiz, R., Scarlata, C., Sluiter, J., Templeton, D., 2008. Determination of Extractives in

530     Biomass: Laboratory Analytical Procedure (LAP), NREL/TP-510-42619.

531 Sraka, M., Škevin, D., Obranović, M., Butorac, J., Magdić, I., 2019. Agroecological conditions of

532     industrial hemp production in the western Pannonian agricultural subregion and fatty acids

533     composition of hemp seed oil. J. Cent. Eur. Agric. 20, 809–822.

534      https://doi.org/10.5513/JCEA01/20.3.2529

535    Struik, P.C., Amaducci, S., Bullard, M.J., Stutterheim, N.C., Venturi, G., Cromack, H.T.H., 2000.

536      Agronomy of fibre hemp (*Cannahis satira L.*) in Europe. Ind. Crops Prod. 11, 107–118.

537      https://doi.org/10.1016/S0926-6690(99)00048-5

538    Tian, S.Q., Zhao, R.Y., Chen, Z.C., 2018. Review of the pretreatment and bioconversion of

539      lignocellulosic biomass from wheat straw materials. Renew. Sustain. Energy Rev. 91, 483–

540      489. https://doi.org/10.1016/j.rser.2018.03.113

541    Upton, B.M., Kasko, A.M., 2016. Strategies for the conversion of lignin to high-value polymeric

542      materials: Review and perspective. Chem. Rev. 116, 2275–2306.

543      https://doi.org/10.1021/acs.chemrev.5b00345

544    Väisänen, T., Kilpeläinen, P., Kitunen, V., Lappalainen, R., Tomppo, L., 2019. Effect of steam

545      treatment on the chemical composition of hemp (Cannabis sativa L.) and identification of

546      the extracted carbohydrates and other compounds. Ind. Crops Prod. 131, 224–233.

547      https://doi.org/10.1016/j.indcrop.2019.01.055

548    Viswanathan, Bharath, M., Cheng, M., Elmo, T., Clemente, Dweikat, I., Singh, V., 2021.

549      Economic perspective of ethanol and biodiesel coproduction from industrial hemp. J. Clean.

550      Prod. 299, 126875. https://doi.org/10.1016/j.jclepro.2021.126875

551    Viswanathan, M.B., Park, K., Cheng, M.H., Cahoon, E.B., Dweikat, I., Clemente, T., Singh, V.,

552      2020. Variability in structural carbohydrates, lipid composition, and cellulosic sugar

553      production from industrial hemp varieties. Ind. Crops Prod. 157, 112906.

554      https://doi.org/10.1016/j.indcrop.2020.112906

555 Wang, Q., Xiong, Y.L., 2019. Processing, Nutrition, and Functionality of Hempseed Protein: A

556      Review. Compr. Rev. Food Sci. Food Saf. 18. https://doi.org/10.1111/1541-4337.12450

557 Xie, C., Gong, W., Yang, Q., Zhu, Z., Yan, L., Hu, Z., Peng, Y., 2017. White-rot fungi

558      pretreatment combined with alkaline/oxidative pretreatment to improve enzymatic

559      saccharification of industrial hemp. Bioresour. Technol. 243, 188–195.

560      https://doi.org/10.1016/j.biortech.2017.06.077

561 Xu, J., Zong, M.H., Fu, S.Y., Li, N., 2016. Correlation between Physicochemical Properties and

562      Enzymatic Digestibility of Rice Straw Pretreated with Cholinium Ionic Liquids. ACS

563      Sustain. Chem. Eng. 4, 4340–4345. https://doi.org/10.1021/acssuschemeng.6b00860

564 Xu, Y., Li, J., Zhao, J., Wang, W., Griffin, J., Li, Y., Bean, S., Tilley, M., Wang, D., 2021.

565      Hempseed as a nutritious and healthy human food or animal feed source: a review. Int. J.

566      Food Sci. Technol. 56, 530–543. https://doi.org/10.1111/ijfs.14755

567 Zhang, K., Johnson, L., Nelson, R., Yuan, W., Pei, Z., Wang, D., 2012. Chemical and elemental

568      composition of big bluestem as affected by ecotype and planting location along the

569      precipitation gradient of the Great Plains. Ind. Crops Prod. 40, 210–218.

570      https://doi.org/10.1016/j.indcrop.2012.03.016

571 Zhao, J., Li, J., Qi, G., Sun, X.S., Wang, D., 2021a. Two Nonnegligible Factors Influencing

572     Lignocellulosic Biomass Valorization: Filtration Method after Pretreatment and Solid

573     Loading during Enzymatic Hydrolysis. Energy and Fuels 35, 1546–1556.

574     https://doi.org/10.1021/acs.energyfuels.0c03876

575  Zhao, J., Xu, Y., Wang, W., Griffin, J., Roozeboom, K., Wang, D., 2020a. Bioconversion of

576     industrial hemp biomass for bioethanol production: A review. Fuel 281.

577     https://doi.org/10.1016/j.fuel.2020.118725

578  Zhao, J., Xu, Y., Wang, W., Griffin, J., Wang, D., 2020b. Conversion of liquid hot water, acid and

579     alkali pretreated industrial hemp biomasses to bioethanol. Bioresour. Technol. 309, 123383.

580     https://doi.org/10.1016/j.biortech.2020.123383

581  Zhao, J., Xu, Y., Zhang, M., Wang, D., 2020c. Integrating bran starch hydrolysates with alkaline

582     pretreated soft wheat bran to boost sugar concentration. Bioresour. Technol. 302, 122826.

583     https://doi.org/10.1016/j.biortech.2020.122826

584  Zhao, J., Yang, Y., Zhang, M., Wang, D., 2021b. Minimizing water consumption for sugar and

585     lignin recovery via the integration of acid and alkali pretreated biomass and their mixed

586     filtrate without post-washing. Bioresour. Technol. 337, 125389.

587     https://doi.org/10.1016/j.biortech.2021.125389

**Table 1**. Mean squares from multi-factor analysis of variance for the effects of genotype, planting location, and their interaction between genotype and planting location on the chemical composition of raw biomass and pH of pretreated and integrated filtrate.

| Source of variation | df | Chemical composition of biomass (%) | | | | | pH of filtrates | | |
|---|---|---|---|---|---|---|---|---|---|
| | | Glucan | Xylan | ASL | AIL | Extractives | HOAc-treated | NaOH-treated | Integrated slurry |
| Genotype | 3 | 13.08* | 2.16** | 0.00 | 5.92** | 23.64** | 0.00** | 0.03** | 0.00 |
| Planting location | 1 | 36.60** | 0.20 | 0.00* | 7.84** | 0.90 | 0.05** | 0.04** | 0.01** |
| Genotype x location | 3 | 2.63 | 0.27 | 0.00 | 1.12 | 5.21** | 0.00** | 0.01** | 0.00* |

ASL: acid-soluble lignin; AIL: acid-insoluble lignin; HOAc: acetic acid; NaOH: sodium hydroxide. Integrated slurry refers to the mixture of pretreated biomass and filtrate. * and ** are statistically significant at $P < 0.05$ and $P < 0.01$ probability, respectively.

**Table 2**. Mean squares from multi-factor analysis of variance for the effects of genotype, planting location, and their interaction between genotype and planting location on the concentration and conversion efficiency of chemicals obtained from simultaneous enzymatic hydrolysis of integrated biomass and filtrate.

| Source of variation | df | Lignin recovery | Chemical concentration (g/L) | | | | Conversion efficiency (%) | | | |
|---|---|---|---|---|---|---|---|---|---|---|
| | | | Glucose | Xylose | HMF | Furfural | Glucose | Xylose | HMF | Furfural |
| Genotype | 3 | 21.00 | 11.64** | 0.74** | 0.01 | 0.16** | 10.62** | 14.23** | 0.03 | 7.51** |
| Planting location | 1 | 172.20* | 12.92** | 0.10** | 0.20** | 0.09* | 6.23** | 0.48 | 0.65** | 10.61** |
| Genotype x location | 3 | 113.17* | 2.30** | 0.46** | 0.03 | 0.02 | 8.12** | 18.80** | 0.18** | 1.33 |

HMF: hydroxymethylfurfural. * and ** are statistically significant at $P < 0.05$ and $P < 0.01$ probability, respectively.

**Table 3.** The conversion efficiency (%, based on original component) and yield (g/kg-biomass) of chemicals obtained from simultaneous enzymatic hydrolysis of integrated biomass and filtrate.

| Biomass | Conversion efficiency (%) | | | | Yield (g/kg biomass) | | | |
|---|---|---|---|---|---|---|---|---|
| | Glucose | Xylose | HMF | Furfural | Glucose | Xylose | HMF | Furfural |
| Haysville | | | | | | | | |
| Anka | 73.40 ± 0.25b | 45.42 ± 0.18a | 2.38 ± 0.15ab | 14.65 ± 1.01b | 405.28 ± 1.37c | 70.47 ± 0.27b | 9.19 ± 0.59bc | 14.53 ± 1.01b |
| Rigel | 74.10 ± 0.18bc | 47.05 ± 0.15a | 2.61 ± 0.04bc | 14.52 ± 0.33b | 405.91 ± 1.00c | 71.08 ± 0.23b | 10.00 ± 0.14cd | 14.01 ± 0.32b |
| Vega | 72.97 ± 0.13b | 45.87 ± 0.21a | 2.39 ± 0.16abc | 12.22 ± 1.23ab | 383.37 ± 0.69b | 69.20 ± 0.32b | 8.82 ± 0.59abc | 11.78 ± 1.19ab |
| Hlukouskii | 75.33 ± 0.19cd | 52.03 ± 0.97b | 2.95 ± 0.02c | 11.14 ± 0.27ab | 418.89 ± 1.05d | 69.20 ± 1.28b | 11.46 ± 0.09d | 9.49 ± 0.23a |
| Manhattan | | | | | | | | |
| Anka | 71.19 ± 0.05a | 46.20 ± 0.09a | 2.13 ± 0.03ab | 12.88 ± 0.57ab | 370.51 ± 0.27a | 68.91 ± 0.14b | 7.76 ± 0.09ab | 12.33 ± 0.55ab |
| Rigel | 75.12 ± 0.77cd | 51.26 ± 0.32b | 2.18 ± 0.08ab | 11.31 ± 0.59ab | 403.84 ± 4.14c | 80.84 ± 0.50c | 8.23 ± 0.32abc | 11.42 ± 0.59ab |
| Vega | 77.71 ± 0.00e | 45.66 ± 0.15a | 2.43 ± 0.14abc | 11.73 ± 0.18ab | 366.85 ± 0.00a | 70.15 ± 0.23b | 7.99 ± 0.45abc | 11.53 ± 0.18ab |
| Hlukouskii | 76.77 ± 0.06de | 45.85 ± 0.00a | 1.96 ± 0.02a | 10.00 ± 0.20a | 396.76 ± 0.32c | 64.04 ± 0.00a | 7.14 ± 0.09a | 8.94 ± 0.18a |

HMF: hydroxymethylfurfural. Data: means ± standard deviations. In each column, means with different letters are significantly different at $P < 0.05$.
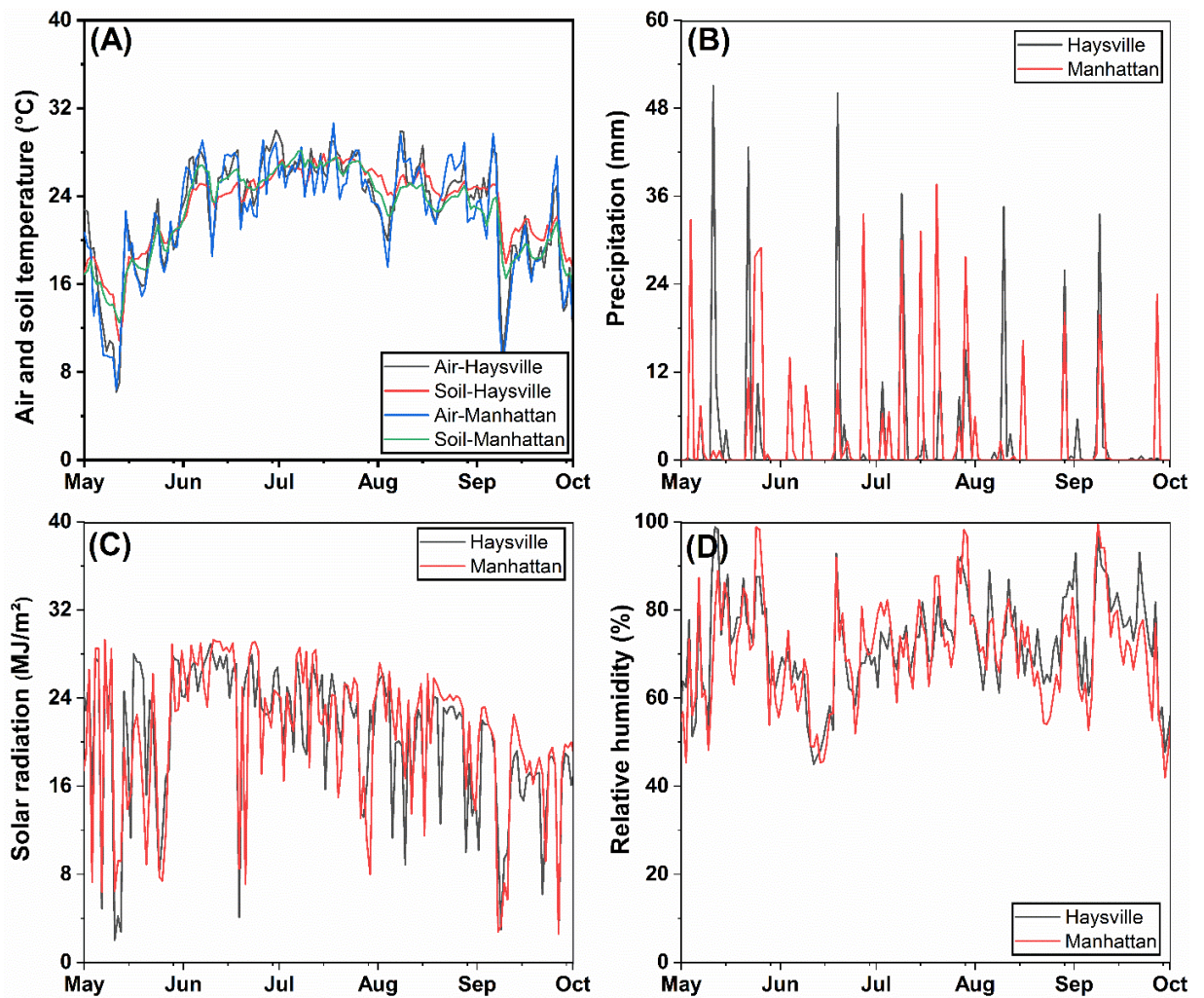
**Fig. 1.** Detailed weather data from May 1st to October 1st (Kansas Mesonet, 2020: Kansas Mesonet Historical Data. Accessed 12 March 2020, http://mesonet.k-state.edu/weather/historical) at Haysville and Manhattan where four genotypes of industrial hemp were cultivated.
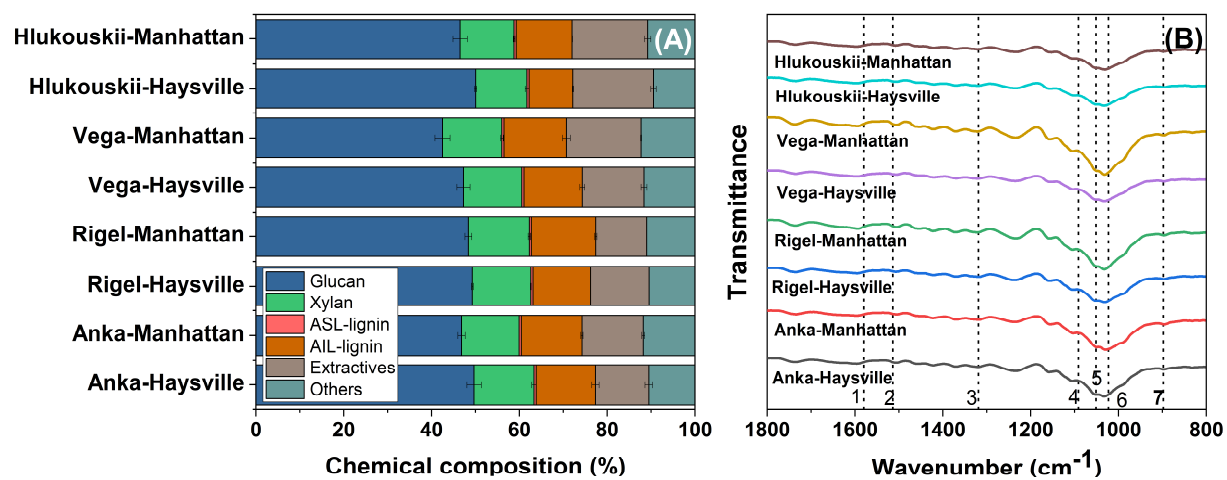
**Fig. 2.** Chemical composition (A) and FTIR spectrum (B) of four genotypes of industrial hemp biomass that were harvested at Haysville and Manhattan (ASL: acid soluble lignin; AIL: acid insoluble lignin).[1]

---

[1]The peaks are denoted as (1) C=C stretching from aromatic skeletal vibration, (2) aromatic skeleton from lignin, (3) syringyl and guaiacyl lignin units, (4) C-O vibration of crystalline cellulose, (5) C-O stretching in cellulose and hemicellulose, (6) C-O-C pyranose ring skeletal vibration ascribed to cellulose, and (7) C-H amorphous cellulose.
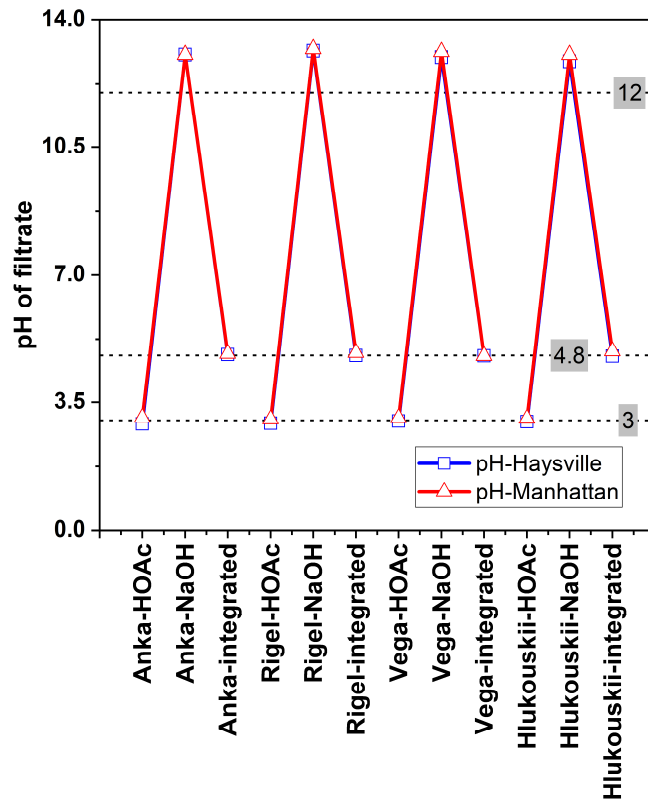
**Fig. 3.** The pH of acetic acid (HOAc) and sodium hydroxide (NaOH) pretreated filtrate before and after the integration process.
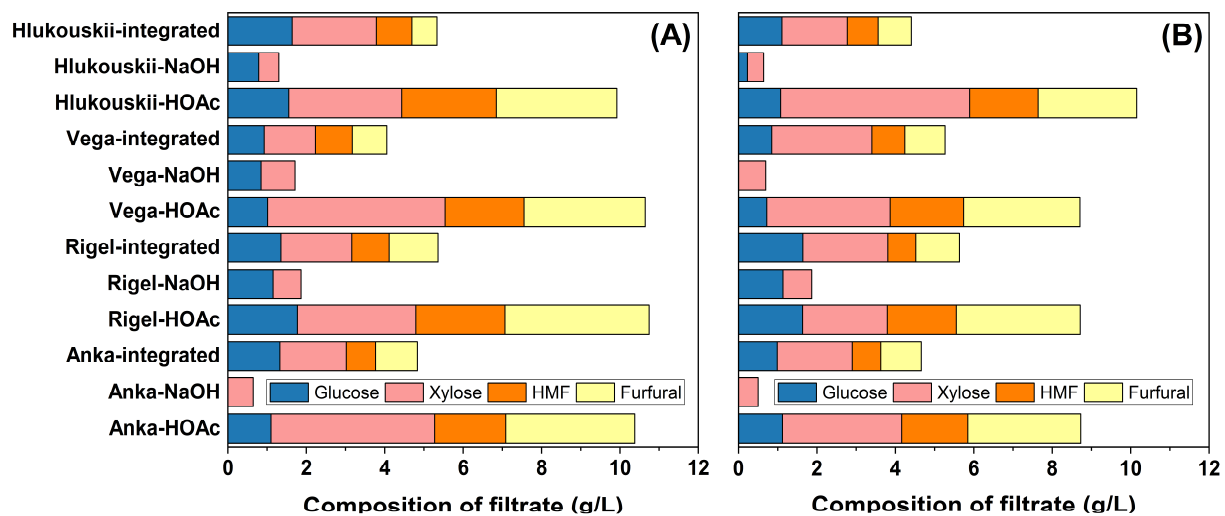
**Fig. 4.** Glucose, xylose, hydroxymethylfurfural, and furfural concentrations in acetic acid (HOAc) and sodium hydroxide (NaOH) pretreated filtrate before and after the integration process (A: Haysville; B: Manhattan).
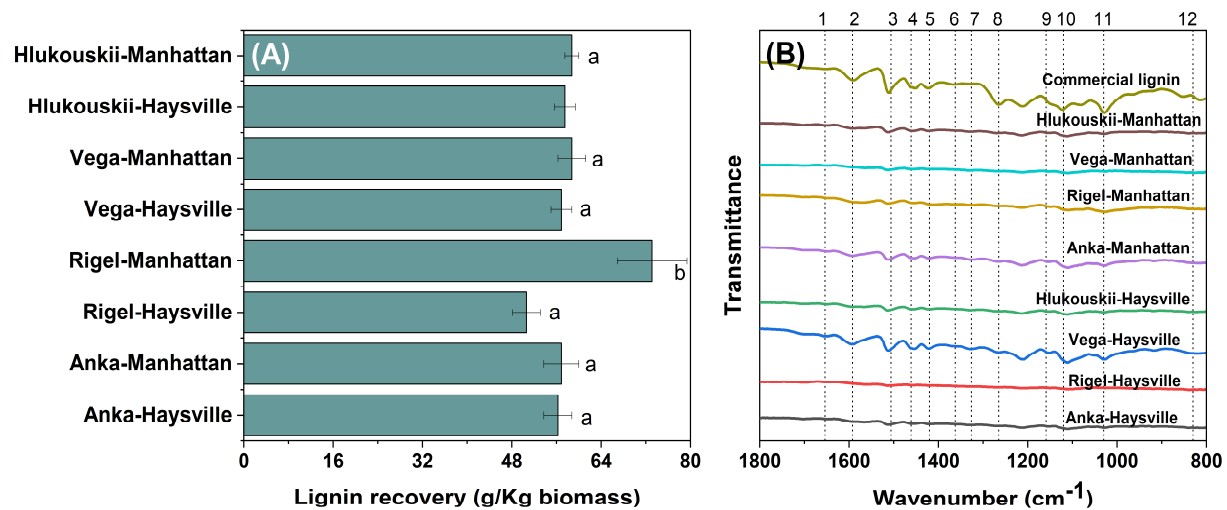
**Fig. 5.** Lignin recovery (A) and Fourier transform infrared spectroscopy characterization (B) with the commercial alkali lignin used as a control. The mean difference is significant at $P < 0.05$.[2]

---

[2]The peaks are denoted as (1) stretching vibrations of conjugate carbonate of carboxylic acid and ketone groups, (2) the vibration of aromatic rings, (3) the vibration of aromatic rings, (4) the methoxyl C-H bending and C-C stretching in the aromatic skeleton, (5) the vibration of aromatic rings, (6) the non-esterified phenolic –OH resulting from the cleavage at α-O-4' and β-O-4' linkage, (7) aromatic C-O stretching of syringyl units and/or condensed guaiacyl units, (8) aromatic C-O stretching of syringyl units and/or condensed guaiacyl units, (9) the p-hydroxy phenylpropane, and (10) the syringyl units, (11) C-OH and C-O-C stretching of the side groups and glycosidic bonds, respectively, (12) the guaiacyl units (Shi et al., 2019).
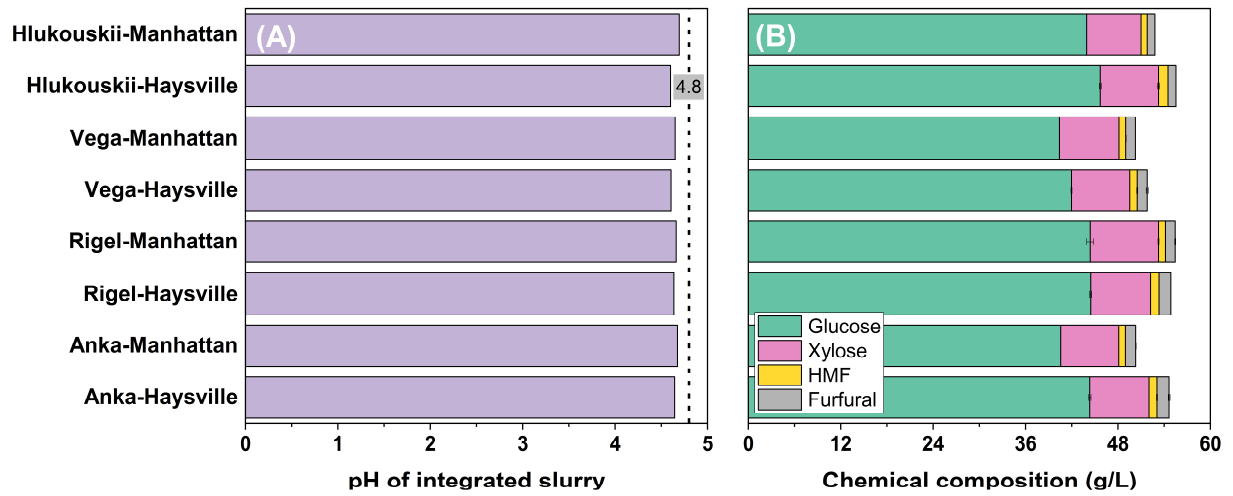
**Fig. 6.** The pH of integrated slurry including pretreated biomass and filtrate (A) and concentrations of glucose, xylose, hydroxymethylfurfural (HMF), and furfural in the hydrolysate after 72-h enzymatic hydrolysis (B).
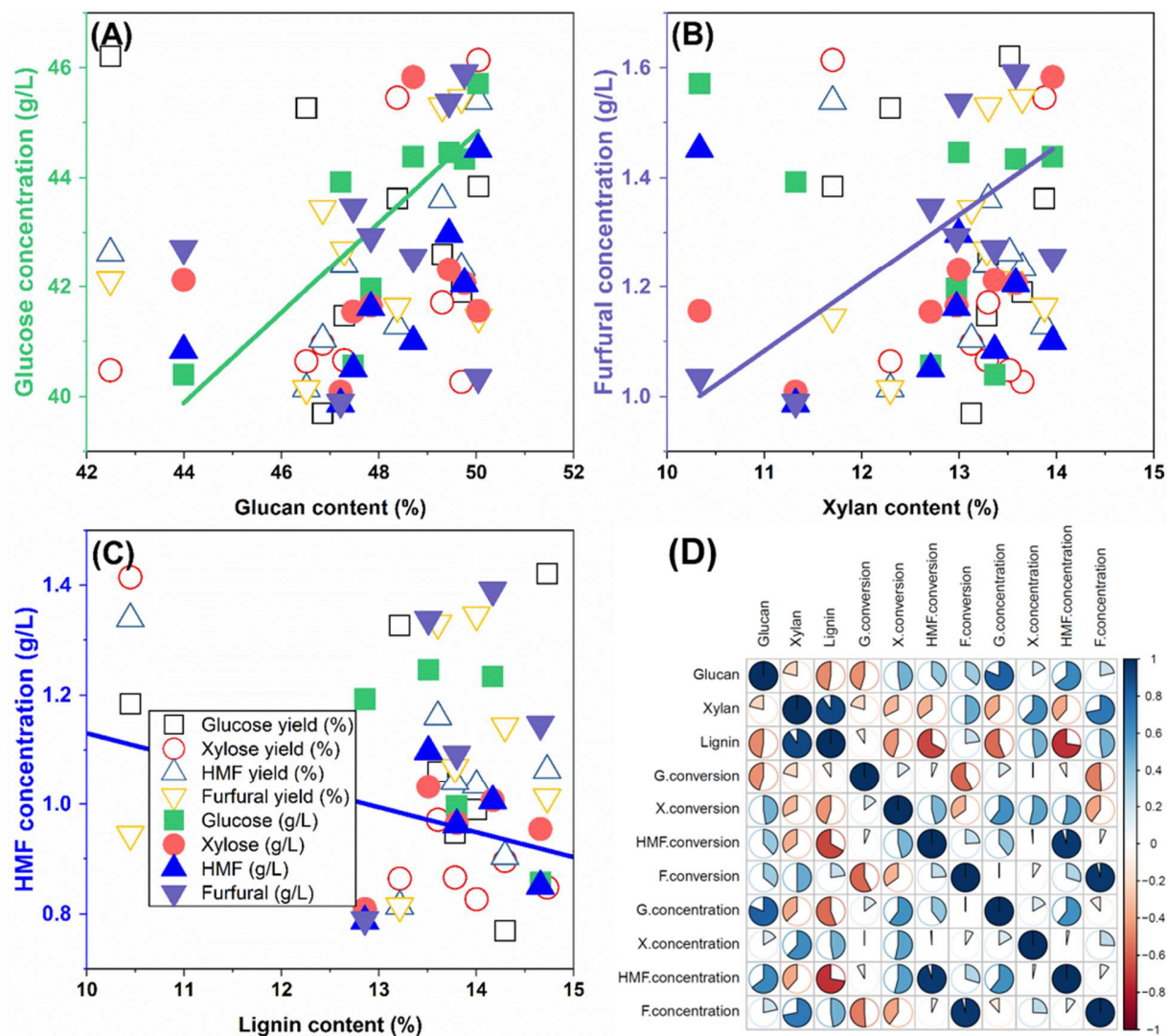
**Fig. 7.** The linear relationships between composition (A: glucan; B: xylan; and C: lignin) of raw industrial hemp biomass and chemical conversion performances as well as correlation coefficients among these parameters (D). The abbreviations are denoted as: G is glucose, X is xylose, HMF is hydroxymethylfurfural, and F is furfural.